Sky Lantern Safety Flight Profile for Risk Assessment

Schuurman, Michiel; Gransden, Derek

DOI
10.2514/6.2017-3289

Publication date
2017

Document Version
Accepted author manuscript

Published in
AIAA Balloon Systems Conference

This is an Accepted Manuscript of an article published in: AIAA Balloon Systems Conference 5-9 June 2017, Denver, Colorado. ISBN: 978-1-62410-495-4
Available online: https://arc.aiaa.org/doi/10.2514/6.2017-3289

Sky Lantern Safety Flight Profile for Risk Assessment

Michiel J. Schuurman[1] and Derek I. Gransden.[2]
Delft University of Technology, Faculty of Aerospace Engineering, Delft, 2629LW

Due to the rise in popularity of sky lantern, research is required to determine the public-safety risk level and its variation as both awareness and usage increase. This work is a first step into a research project to quantify the risk of very low level operational airspace impact and potential ground-fire posed by sky lanterns. In order to achieve this goal, this paper details a linearized model of the sky lantern vertical flight profile based on ground-level experimental results. A sample of five different types of sky lanterns, in three shapes with different volumes, were used in full-scale laboratory experiments, to obtain quantitative data to determine the sky lantern buoyancy force. By combining the dynamic hot air balloon model found in literature with experimental research data as a reference, a linear dynamic model describing the vertical flight profile of a sky lantern was generated. This dynamic model will subsequently be used for future research to quantify the sky lanterns' potential safety risks, such as the likelihood of impact with low-flying aircraft, interactions with tall structures, and the potential for initiating forest or grass fires by touching down while still aflame.

Nomenclature

a	=	vertical acceleration, m/s^2
c_d	=	aerodynamic drag coefficient ascent phase
D	=	aerodynamic drag, N
g	=	acceleration due to gravity, g = 9.81 m/s^2
h	=	height, m
L	=	aerostatic lift force, N
L_∞	=	lapse rate of air = 6.5×10^{-3} K/m
M	=	molar mass of air = 0.02896 kg/mol
m	=	mass as a function of time, kg
m_0	=	mass of balloon structure at ignition, kg
m_{final}	=	final balloon mass being accelerated, kg
m_{tot}	=	total mass of balloon (in reference equations), kg
P_i, P_∞	=	internal (within the balloon envelope), external air pressure, Pa
P_0	=	measured ground pressure, Pa
R	=	air gas constant = 8.314 J/mol·K
$\tilde{r}$	=	radius of cylinder of equivalent volume to sky lantern, m
t	=	time, s
T_i, T_∞	=	internal (within the balloon envelope), external air temperature, K
T_0	=	measured ground temperature, K
u	=	velocity (positive -up), m/s
V	=	volume balloon, L
W	=	weight balloon, N
ρ_i, ρ_∞	=	internal (within the balloon envelope), external air density, kg/m^3

[1] Assistant Professor, Aerospace Structures & Materials Department, Faculty of Aerospace Engineering, Delft University of Technology, Kluyverweg 1, 2629 HS Delft, The Netherlands, non-member.
[2] Assistant Professor, Aerospace Structures & Materials Department, Faculty of Aerospace Engineering, Delft University of Technology, Kluyverweg 1, 2629 HS Delft, The Netherlands, non-member.

CFR – Code of Federal Regulations (USA)
NFCPSA – Netherlands Food and Consumer Product Safety Authority
RNMI – Royal Netherlands Meteorological Institute (KNMI)
VWA – Voedsel en Waren Autoriteit (NL) - NFCPSA (EN)

I. Introduction

Manned hot air balloons were constructed to lift humans and were recorded as successful by the late seventeenth century in France. The development has continued since then, and hot air balloon flight is becoming increasingly popular. Various research has been conducted on hot air balloons, including the use of inflatable balloons to reach the boundaries of space and even on other planets. Nevertheless, the principle of the hot air balloon has been known to the Chinese since ancient times; small-scale hot air balloons called "Chinese lanterns" or "sky lanterns" were used on the battlefield for communication between troops. Peaceful applications of sky lanterns usage are mainly for celebrations, such as the Chinese New Year, the Mae Jo, or Yi Peng festivals, where thousands of sky lanterns are simultaneously launched.

In Asia, sky lanterns have been made for centuries as part of long-established tradition for luck and prosperity. In The Netherlands and around the world, the sky lantern is gaining popularity and can be seen to drift across the sky more often following weddings and during New Year's celebrations. Consequently, with the increase in the popularity of sky lanterns, their availability to the public has increased, and sky lanterns can be purchased online and in specialty stores in many countries. The cost of a single sky lantern is already very low, generally a few dollars, and when bought in bulk the unit price starts to decrease further, dually making the sky lantern more attractive for celebrations and increasing the probability of multiple sky lanterns being released simultaneously. Safety concerns related to the use of sky lanterns have been increasingly debated as the open flame, which is used for lifting the sky lantern, is uncontrolled and can potentially ignite large forest fires or man-made infrastructure.

Additionally, conflicting statements about the height and flight duration of the sky lantern exist between manufacturers and regulating safety bodies. According to manufacturers, sky lanterns can reach a height of up to 1 mile (1600 meters) altitude, whereas some estimates, based on researched published by a Dutch government agency called the Nederlandse Voedsel en Waren Autoriteit (NVWA - The Netherlands Food and Consumer Product Safety Authority - NFCPSA), consider the achievable height to be on the order of only a few hundred meters[1].

The research goal for this project is to comprehend and quantify the risk posed by sky lanterns and their interaction with low level flying aircraft. In order to achieve this research goal, the first step is to model the sky lantern vertical flight profile (height) and determine the maximum altitude these unmanned, uncontrolled aerovehicles can obtain. For this purpose, a limited series of full-scale laboratory experiments was undertaken to determine the sky lantern buoyancy force as a function of time. By combining a dynamic balloon model found in literature with experimental data as input, a model describing the vertical flight profile of a sky lantern was generated. Due to the variability in size and shape of sky lanterns available in The Netherlands, a total of five sky lanterns types, representing a spread of envelope volumes and shapes, were investigated.

In this paper, a sky lantern is defined as a lightweight, open-flame impregnated rice or mulberry paper body, forming a balloon envelope attached to a bamboo frame at its base. Typically, a cloth saturated with (paraffin) wax comprises the burner that hangs in the center of the round bamboo frame, attached by two perpendicular diametric strings. The bamboo base has a secondary function, which is to preserve the balloon shape to facilitate the ingress of hot air in the envelope. Below the burner cloth patch, a woven fire-resistant sleeve is attached to protect the user from droplets of combusting liquefied wax or paper during the sky lantern launch and to keep the burning fuel cell off the ground upon landing. In some sky lantern designs, the burner is attached to an upper frame; and a lower frame, three centimeters below the upper frame, prevents the burner from hitting the ground upon landing. There are no other safety devices included onboard the sky lantern, and it is dependent upon the user to properly follow the instructions and warnings on the packaging.

II. Sky lantern regulation

The sky lantern construction and material are very different from the nominal engineering hot air balloon and other lighter-than-air vehicles. In the United States of America, hot air balloons, or manned free balloons, are regulated by Part 31 of the Title 14 Code of Federal Regulations (CFR), Airworthiness Standards: Manned Free Balloons[1]. Thus, manned free balloons have requirements on the structure, performance, operation, and safety concerning their use. Part 101, Subpart D - Unmanned Free Balloons[2] is more appropriate for a sky lantern.

However, in this Part of the CFR, no structural nor performance requirements are described, except for some operational limitations. For instance, the government does stipulate the sky lantern should be held before launch for at most two minutes. For a sky lantern, no structural nor performance regulations exist; therefore, it is effectively an unregulated balloon.

In several countries, sky lanterns are deemed to pose an environmental risk and could possibly hurt wild or domesticated animals, which has resulted in a ban. In particular, this resulted from previous iterations of commercial sky lanterns that used metal wires in their construction, which livestock ingested and frequently resulted in the euthanasia of the animals. In many countries, like The Netherlands, the regulator has chosen to put rules in place to warn the public and restrict the operational use. For instance, an operational limit is given for the maximum wind speed that is allowed during launch[3]. A second operational limit is the launch site location, which is required to be at least 10 kilometers from an airport. Although these regulations are in place, the operability in practice is likely to be driven by occasion, and users do not adhere to limits set by the government. In such cases, infractions are rarely reported or enforced, and punishment improbable. Therefore, a currently unassessed probability of fire or damage to environment and infrastructure remains.

III. Previous research

For this paper, a literature review was performed to examine previous research conducted on sky lantern performance and trajectory modeling. It was determined that no scientific research has been published in this area. However, as sky lanterns are similar to hot air balloons, the literature review focused on the examination of hot air balloons. Furthermore, the performance and modeling of high altitude and extraterrestrial were excluded from this review as sky lanterns would not fly beyond the troposphere.

Hot air balloons have historically been used in, for example, atmospherical research, telecommunication research and aerial surveying. Some of the early work on modeling for atmospherical research balloons was done by Kreider[4] and Stefan[5]. Their models took into account thermodynamic influences of solar and infrared radiation, as well as optical/infrared absorptivity and related radiative properties of balloons. In 1975, the Scientific Ballooning Handbook[4] was published, describing the hot air balloon equations of motions and energy balance. By using these equations, numerical computer programs were developed that could predict the hot air balloon trajectory[7].

A vertical dynamic hot air balloon model was developed by Ellenrieder[8] in 1999. This paper was aimed to develop a model of the vertical motion of a hot air balloon and verify the model results by conducting several flight tests. This research was the first step in developing an altitude–hold autopilot for a hot air balloon. In this paper, it was concluded that the developed model had sufficient fidelity for the proposed dynamic modelling needed in the development of flight control systems. However, further areas of model improvement are highlighted, which would extend the applicability of the balloon model. The study highlighted the improvements of cooling and drag, which could improve the model accuracy.

In 2009, the NFCPSA conducted several tests to determine the sky lanterns' performance. The NFCPSA requested the Royal Netherlands Meteorological Institute (RNMI), who launches a weather balloon each day for meteorological measurements, to experimentally estimate the maximum visible altitude of the sky lanterns. The weather balloons that the RNMI normally launches are not sky lanterns; however, the expertise of the personnel involved was used to acquire an estimate of the sky lantern height and distance traveled after launch in their own study. Several uninstrumented flight tests were conducted to evaluate the flight profile of the sky lanterns during their ascent. The flight tests were conducted on the premises of the RNMI at De Bilt. Therefore, the height and distance estimations, see Table 1, were not corroborated by measured data.

Table 1: NFCPSA Height and distance data[1]

Flight Number	Approximate Flight Duration [s]	Approximate Height [m]	Approximate Distance [m]
1	180	200	950
2	300	300	1580
3	240	300	1266
4	300	200	1580
5	240	300	1900
6	120	50	633
7	180	150	950
8	180	100	950
9	120	100	633
10	180	60	950

IV. Sky lantern mathematical model

Assuming that a sky lantern is a free-floating unmanned balloon, comparable to a hot air balloon but without the additional passenger load, the sky lantern analytical modelling can be based on the hot air balloon equations of motion described in previous work. The equations for the vertical dynamics of a balloon have been described in several papers[4-6]. The acceleration of a hot air balloon is based on Newton's Second Law and Archimedes' Principle governing buoyancy. Some of the simplifying assumption used in the mathematical representation are:

- The internal pressure and temperature are uniform over the volume of the envelope. Unlike other papers, the total mass term is not constant, but the mass loss of the burner is constant, and the mass of the hot air contained within the envelope is constant.
- Further, the shape of the sky lantern does not affect its kinetics, and the envelopes can be approximated as equivalent cylinders (that is, the cross-sectional area of the sky lantern is constant).
- The variation of air pressure, density, and temperature is not constant, but the values of the pressure, density, and temperature can be interpolated from standard atmospheric tables.
- The drag always acts to slow down the motion of the sky lantern, and therefore, is applied as an absolute value decay.
- The pressure difference between the opening in the envelope (the underside) and the outside air is negligible and the mass/heat flow between the inside of the envelope and out is not considered.

A. The ascent phase model

Starting with the equilibrium forces, as the measurements were the buoyancy forces measured at a constant atmospheric temperature and pressure, the equation of motion in the vertical direction can be described as

$$L - W - D = m_{tot} a_{ascent}, \tag{1}$$

where positive is assumed upward, and drag acts downward in ascending flight. However, the aerostatic lift is given as

$$L = (\rho_\infty - \rho_i) g V, \tag{2}$$

where the density of the outside air can be computed based on the Ideal Gas Law and the atmospheric standard conditions as a function of altitude. The Ideal Gas Law state equation for the external air is given by:

$$\rho_\infty = \frac{PM}{RT}, \tag{3}$$

and the variation of pressure and temperature with altitude in the troposphere are given as

$$P = P_0 \left(1 - \frac{Lh}{T_0}\right)^{\frac{gM}{L_\infty R}}, \tag{4}$$

and

$$T = T_0 - L_\infty h, \tag{5}$$

where the dependence on altitude is given by the variable h, in meters and the measured ground value is denoted by the naught symbol.

Since the pressure difference between the opening at the bottom of the envelope and the outside air is negligible ($P_\infty \approx P_i$), the standard lift equation of a balloon is given by combining Eqs. 2-5 into Eq. 6:

$$L = \left[\left(\frac{P_0 M}{R T_0}\right)\left(1 - \frac{Lh}{T_0}\right)^{\frac{gM}{L_\infty R}-1} - \rho_i\right] g V, \tag{6}$$

so the dependency of the lift as a function of height is based also on the measureable ground pressure and temperature.

The drag term in Eq. 1 can be found from literature[7]; however, in the present case, the dependency of the external air density is also considered to be a function of the altitude:

$$D = \frac{1}{2}\left[\left(\frac{P_0 M}{RT_0}\right)\left(1 - \frac{Lh}{T_0}\right)^{\frac{gM}{L_\infty R}-1}\right] Ac_D u|u|, \tag{7}$$

where the area is based on the equivalent circular area given as $A = \pi\tilde{r}^2$, and $\tilde{r}$ is the radius of a sphere with an equivalent volume of the sky lantern. The direction of the drag is determined by the direction of the velocity of the sky lantern.

Depending on the sky lantern type, approximately 30% of the weight is the fuel cell. However, the sky lantern mass changes due to fuel burning. As such, the sky lantern weight is a dynamic factor depending on time. Therefore, the mass loss was calculated based on a start and end weight of the sky lantern with a linear approximation based on time between alighting the fuel cell and the flame-out condition. The total mass, including the hot air inside the envelope, is given in the form of:

$$m(t) = m = m_0 - \Delta m. \tag{8}$$

and the mass can otherwise be given as a function of height, if the relationship between height and time is known.

The final equation to be solved is then

$$[\rho_\infty - \rho_i]gV - \frac{1}{2}\rho_\infty Ac_D \frac{dh}{dt}\left|\frac{dh}{dt}\right| = m\left(g + \frac{d^2h}{dt^2}\right), \tag{9}$$

where

$$\rho_\infty = \left[\left(\frac{P_0 M}{RT_0}\right)\left(1 - \frac{Lh}{T_0}\right)^{\frac{gM}{L_\infty R}-1}\right], \tag{10}$$

which is a second-order differential equation on position (height) only.

B. The descent phase model

The descent phase sky lantern model is based on the moment when the buoyancy force is neutral, and no longer drives the upward motion of the sky lantern. To simplify the descent phase, the assumption that the sky lantern falls freely after the burner is out is applied. Then the kinetics can be reworked from Eq 1., but without the lift term. Therefore, the equation of motion for the descent phase is

$$a_{descent} = \left(\frac{D}{m_{final}}\right) - \left(\frac{W}{m_{final}}\right) = \frac{1}{2}\rho_\infty Ac_D \frac{dh}{dt}\left|\frac{dh}{dt}\right| - g. \tag{11}$$

For the descent phase, it is assumed that after the combustion of the fuel patch the sky lantern mass is constant. The descent phase can be described as an initial acceleration after which the sky lantern will fall with a constant terminal velocity to the ground.

V. Static performance experimentation

Two factors contributed to the difficulty of accurately measuring the buoyancy forces with the sky lanterns. The first is that the low mass of the sky lantern meant that the measurements had to be recorded as non-intrusively as possible to prevent interference and false performance measurements. The second is that the range of the measurements is only on the order of decanewtons and the resolution needed to be on the order of at most decinewtons. The measurements had to be sensitive to moderate-frequency and small sample changes, to have an accurate numerical model. Initial testing showed that some of the available high-accuracy equipment could measure in the required force range (up to 10 N), but required an elaborate connection arrangement, which exceeded the sky lantern lifting force and prevented the sky lantern from lifting off the supports.

After several iterations, the simplest measurement provided consistent results: the sky lanterns were attached with light string to known masses atop a sensitive digital balance scale. The sky lanterns were placed with just-slack strings on steel arms clamped to a retort stand, so that the sky lantern was raised approximately 20 cm above the testing surface to prevent interference, and to be able to show lift-off when the buoyancy force of the envelope exceeded that of the weight of the entire system. The entire rig was placed in a fire-proof overhead ventilated lab

with no lateral airflow to minimize the outside influences (Figure 1). A digital video recorder was used to record the ignition time, the moment of lift-off, the time of touch-down on the stand (neutral buoyancy), and the time to flame-out. It should be noted that in this case, the 'touch-down' time is not the time that the sky lantern would hit the ground, but the time that the buoyancy forces could no longer accelerate the sky lantern upwards. (This time, therefore, would correspond with the maximum altitude achievable by the sky lantern *if* no atmospheric thermal, pressure, or density effects were considered.) Flame-out was the time at which no flame was visible, although an infrared camera captured residual heat from the burner patch, but after which the burner was considered inactive. The time for flame-out was recorded so that the total mass loss of the initial package (without the mass of the heated air) could be considered, and the total time of the sky lantern mass loss could be defined. It was assumed that the exhaustion of the fuel caused the flame-out, which meant that no further reaction, and therefore no additional significant mass loss, occurred.

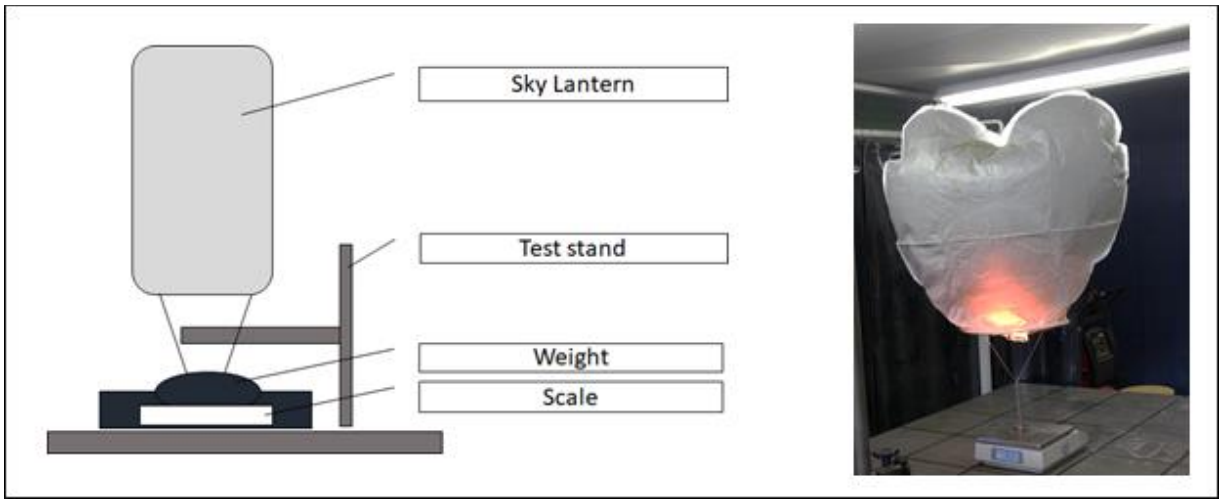

Figure 1. Schematic overview of static test set up (left), sky lantern measurement Type B Heart (right - not shown: thermal camera, video recorder)

The results were compared to another test setup, which is not included in this paper, which rigidly attached the sky lantern with known masses to a scale. The lift profile could then be compared and verified with the original test setup, in the case there might be mismeasurement due to the extension of the strings. Since the average flight duration and the average lift force was attained by both setups, only the testing regime with the first setup (strings) is covered in this paper.

The static tests were performed on five (5) different types of sky lanterns, with varying volumes and envelope shapes, all listed in Table 2. During the test campaign, a total of 38 sky lanterns were tested, although, due to the availability of the lanterns, some types were tested more frequently than others. The tests conducted for this paper were done following manufactures instructions, except for the fact that they were done inside to have the most undisturbed and repeatable flight conditions. Ground temperature and atmospheric pressure were also recorded for each test, but over the course of the testing the variation of the temperature and pressure was less than one percent of the baseline standard atmosphere at room temperature.

Table 2: Sky lantern research type designation and characteristics

Type	Shape	Envelope Volume [L]	Average mass [g]	Mass std. dev. [g]
A	Pear	125.5	53.55	1.07
B	Heart	104.6	59.32	1.55
C	Cylinder	165.8	87.85	3.42
D	Heart (XL)	239.8	113.78	1.92
E	Pear (XL)	194.0	90.32	1.25

VI. Sky lantern measurement and static performance test results

A. Inspection of sky lantern and mass before ignition and after flame-out

Examination and inspection of the sky lanterns used in this research showed that quality control and product consistency was low. Large differences in the masses and quantity of envelope material were present, even between sky lantern types from the same manufacturer. Additionally, many minor holes and tears in the impregnated rice paper were noted during the inspection prior to ignition of the burner. The burners or fuel patches were often not well-aligned with the center of the envelope, which made consistent experimenting difficult.

Type C sky lanterns, those constructed with a double bamboo safety ring, had cardboard inserts to keep a pre-determined separation between each ring; however, these inserts were flimsy and often did not function well. Despite all the manufacturing flaws, the greatest influence was the presence of holes or tears near the top of the envelope, where heat could most easily escape.

Another influencing factor appeared to be the burner mass; although the ratio of mass before and after burn is fairly consistent for each type of sky lantern, as shown in Figure 2, the initial mass of the burner seemed to dictate the total impulse (the integration of the force curve over time) applied to the sky lantern.

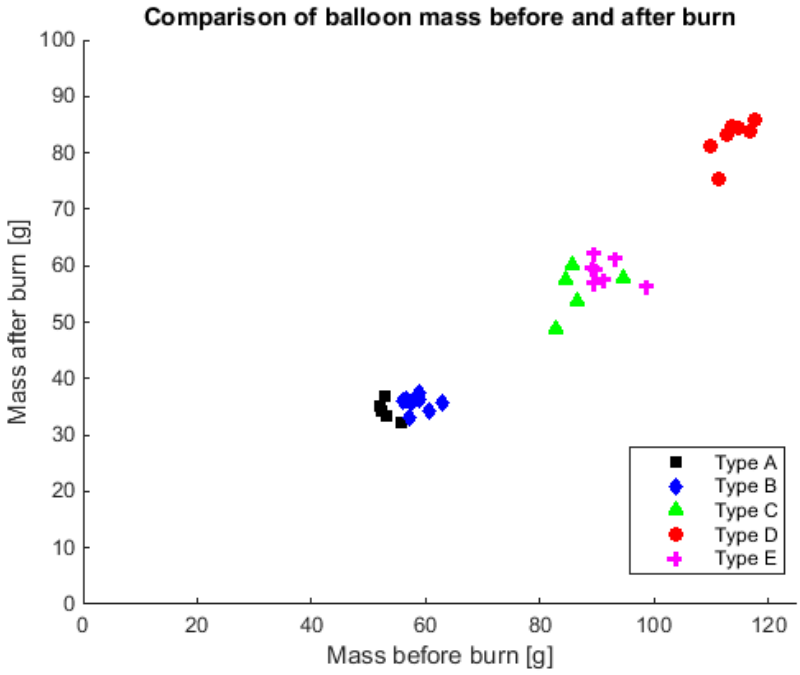

Figure 2. Sky lantern mass measured before burn and just after flame-out

B. Measured lifting (buoyancy) force at ground level

The burner of the sky lanterns, which consisted of square layers of cloths permeated with paraffin wax, were not aligned evenly in all sky lanterns, and exhibited varying burn patterns. Thus, the heat flux was affected by the combustion of the fuel, and the potential buoyancy force (as a function of time) attained was inconsistent. Generally, this was a greater concern with the larger sky lanterns (Type C and D) than with the smaller ones (Type A and B). Several examples in Figure 3 show a dip (Type C and D) in the force after initial lighting, but then the peak value is delayed in the force history plot. These trends resulted from a lack of complete ignition of one corner of the patch, for instance, if a side self-extinguished, causing lower heat flux. Adjacent layers did not always ignite smoothly, which may explain the delay in some of the peak buoyancy forces in the force-time plots.

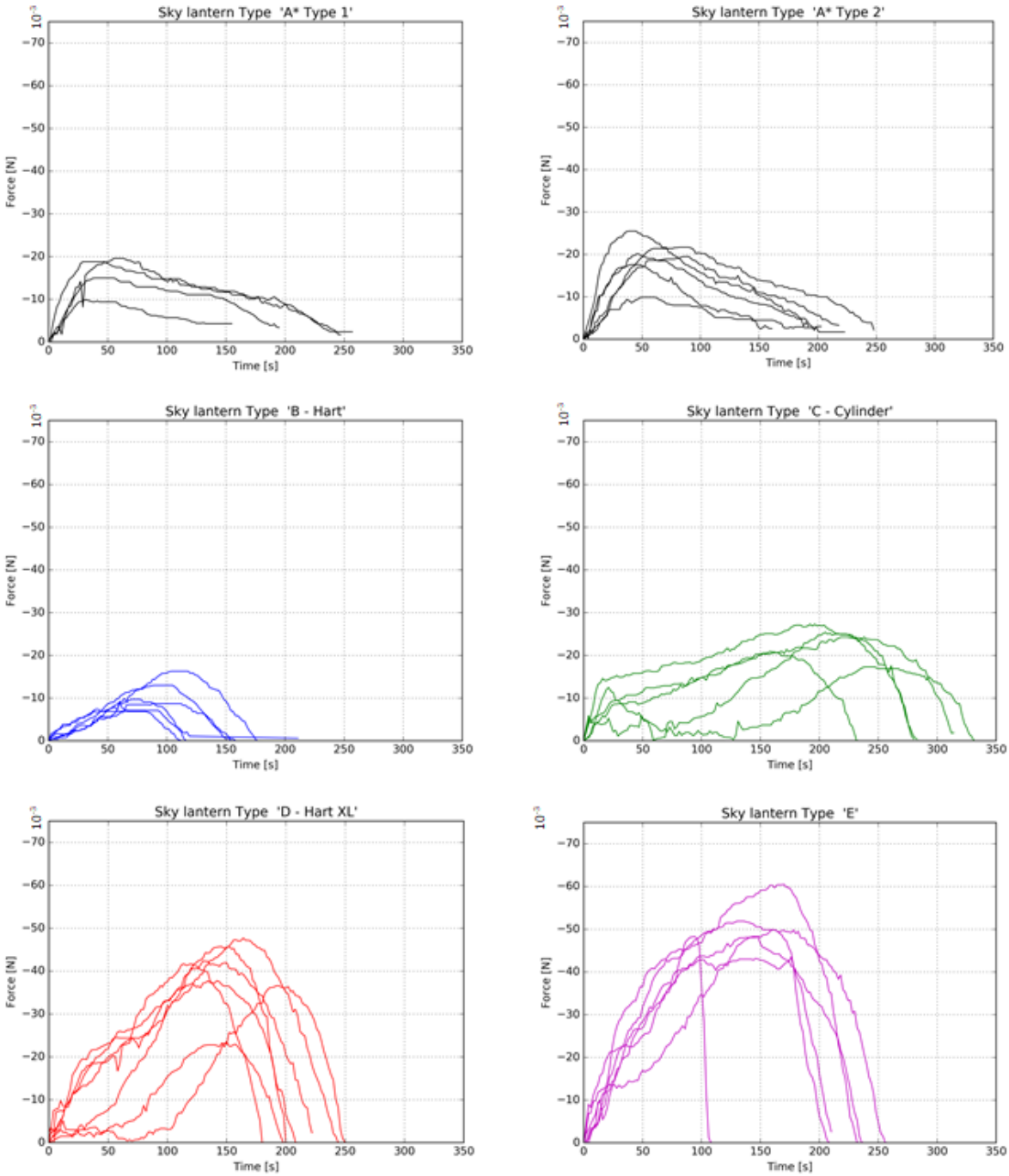

Figure 3. Measured lifting (buoyancy) force at ground level for five types of sky lantern (Note: force is negative because the difference in mass on the scale was recorded.

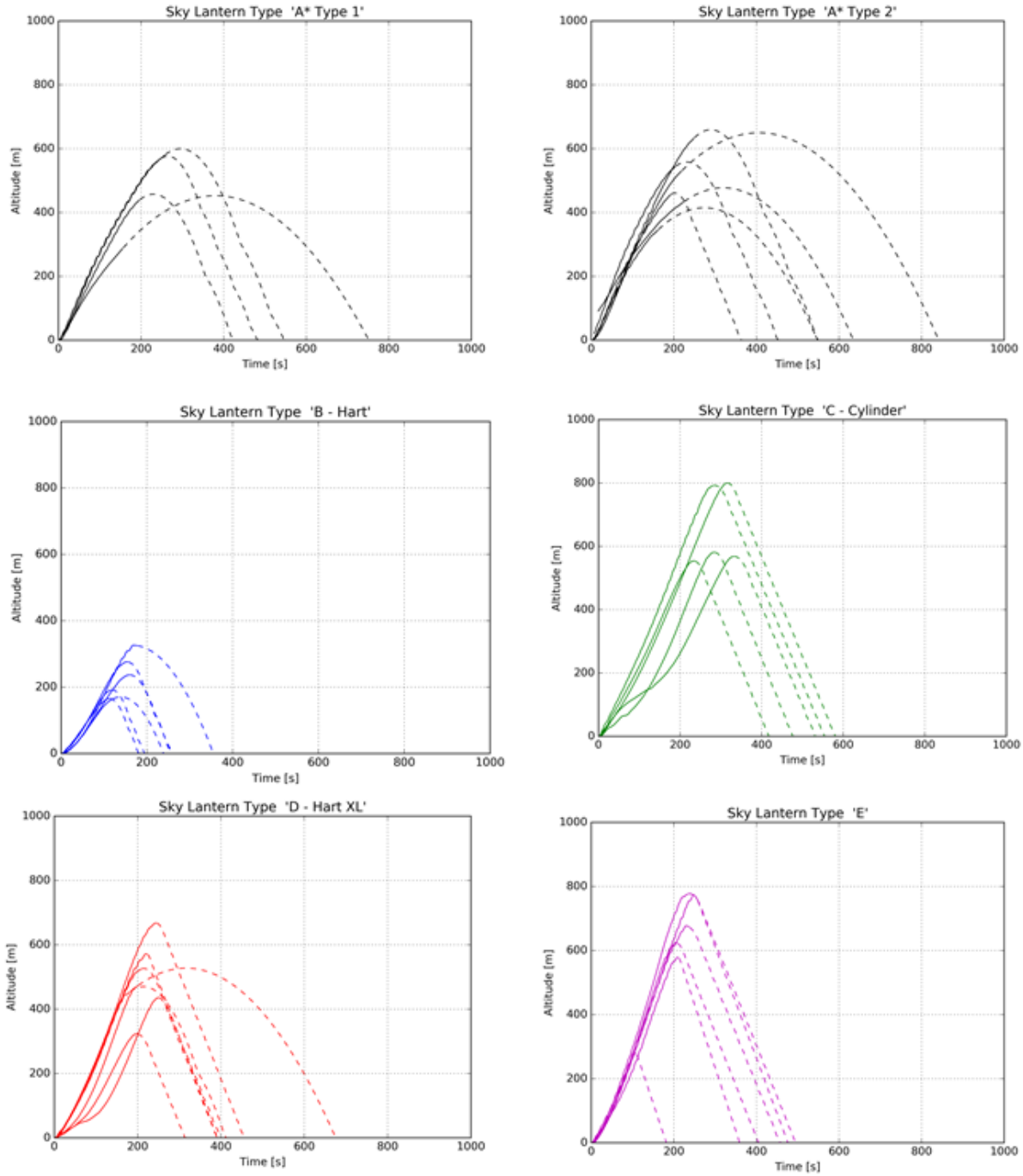

Figure 4. Calculated altitude and flight duration for sky lantern types

VII. Discussion

A. Comparison of altitude performance of sky lantern types

As can be seen in Figure 3, the force-time curves are quite variable between types of sky lantern, and also within each category and size of sky lantern. For instance, Types A and B (pear and heart) had similar volumes, and they achieved similar maximum forces, however, the impulses for Type B are approximately half those of Type A. This results primarily due to the duration of the burn: Type B lasts a little more than half the time of Type A. Additionally, Type A and Type B had impulse profiles that were inverted with respect to each other: Type A sky lanterns tended to burn faster initially and dissipate slowly, while Type B tended to burn slowly and extinguish quickly. The smaller sky lanterns burned for at least 100 s, although the average of Type A was approximately 200 s. The cylindrical sky lanterns, Type C, had the longest burn times, even though both Type D and Type E had greater envelope volume. However, there are some outliers in the experimentation, which are exemplified by the failure of one Type E sky lantern. During one test, the crown of the sky lantern caught fire and it opened up, releasing smoke and hot air, causing the sky lantern's upward force to suddenly drop to zero after only 105 s. With such a large opening in the envelope of the sky lantern, no buoyancy could be preserved.

To calculate the altitudes of the sky lanterns as a function of time the measured lifting force was used as an input to the formulas and analytical models described in Section 4. The measured data from Figure 3 were iteratively corrected for the density as a function of the height in the atmosphere, and using the ground pressure and temperature as inputs. (The ground pressure and temperature were measured in the laboratory at the Delft University of Technology, which is at sea-level.) To model the drag, a value of $c_D = 0.3$ is adopted. For each group of sky lanterns, the altitude as a function of time is plotted in Figure 4.

In a couple of cases, particularly for Type C and Type D, the burn was uneven and delayed, which increased the flight duration and height. This was due to the fact that an increase in buoyance was created at a later movement in time – automatically increasing the duration of the flight and also affecting the maximum height. Therefore, it seems beneficial to delay the combustion of fuel, perhaps by lighting only one corner of the fuel patch, which will increase the maximum height.

Figure 5 shows a boxplot of the altitude for each of the sky lantern types, with the quartile range and the maximum and minimum altitudes modeled from Figure 4. From Figure 5, it is clear that the sky lanterns that tend to achieve the highest altitudes are those with the larger volume envelopes and larger burner masses. The envelope shape affects the maximum altitude when comparing similar volumes. For instance, heart-shaped sky lanterns perform poorly compared to the cylinder or pear shape, even in the case of Type D relative to Type C, which has a much greater volume and larger burner mass.

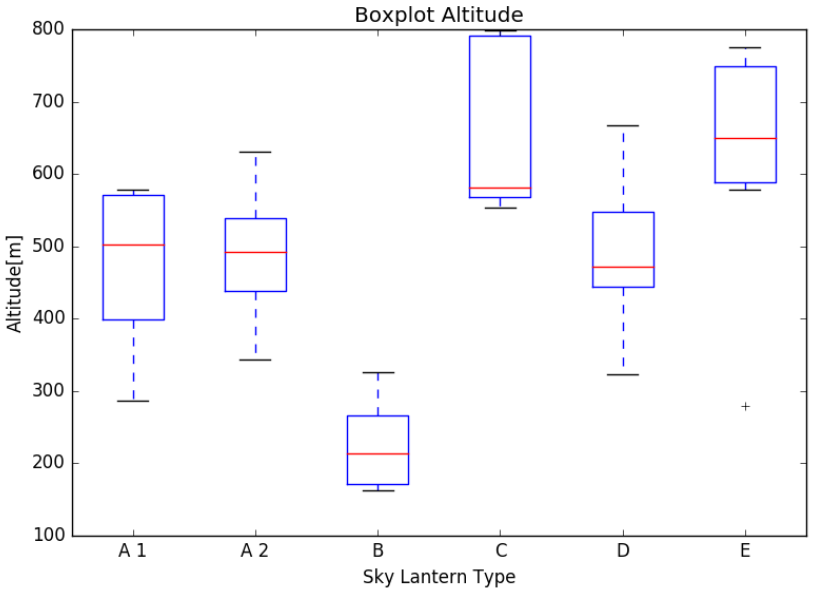

Figure 5. Boxplot of sky lantern type and calculated altitude performance

The mass of the sky lanterns varied by more than 10% for some types, although the trend in Figure 2 shows an approximately linear relationship between the type of sky lantern and its start and end mass. Therefore, it is conceivable that knowing the shape and the fuel cell mass, provided the fuel cell is a cloth patch saturated with paraffin wax and the construction of the sky lantern is of impregnated rice paper with bamboo reinforcement, an estimation of the sky lantern average altitude can be calculated. Figure 6 shows the relationship between the fuel cell mass, shape, and the height performance of the sky lanterns. The figure shows that the mass of the fuel cell does increase the possible height, if one compares the small pear (Type A) and larger pear (Type E) shapes, but the fuel cell mass has a greater influence on the heights of the small heart (Type B) relative to the large heart (Type D). It seems the more regular the shape, particularly its slenderness, the higher the achievable altitude; although, as the height (and surface area) of the envelope increases, so would the heat loss through the impregnated rice paper, which would reduce the performance of the sky lantern.

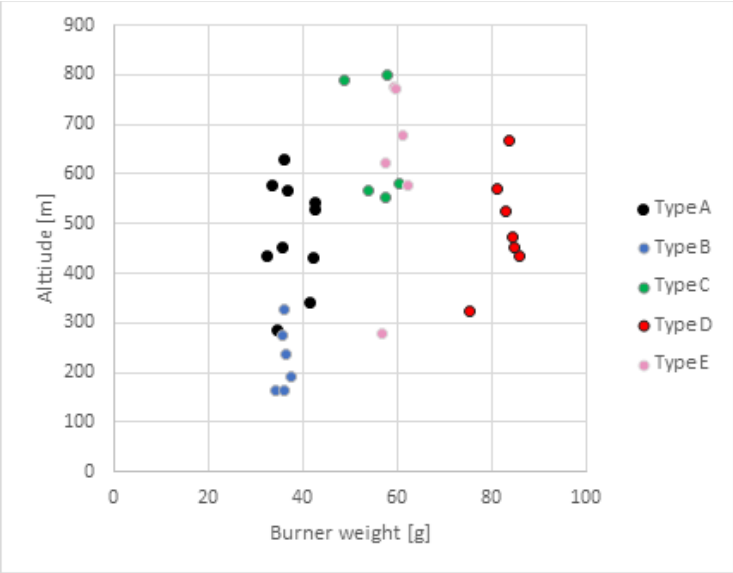

Figure 6. Comparison of burner weight and altitude performance of sky lantern types

It is important to note that the heights achieved by all sky lanterns can interfere with very low level flying aircraft operations. According to the current model, the sky lanterns should be able to achieve a height greater than the estimates from the NFCPSA, which are tabulated in Section 3. It should also be noted that the actual flights conducted by the NFCPSA were *in situ*, (hence, with wind and varying atmospheric temperature/pressure conditions), and therefore, these flights may better represent the sky lanterns' common operational envelope, not the achievable limits. Therefore, a more in-depth analysis, with a thermal model and validated flight testing is recommended, since the interactions with public unmanned aerial vehicles (such as quadcopter drones) or manned aircraft can occur.

B. Comparison of flight duration of sky lantern types

The comparison of the flight duration is interesting from a safety perspective, because there is a hazard in open, uncontrolled flame impacting the ground before it is extinguished. In general, the burn times measured were longer than was reported by the NFCPSA. (The current experimental research recorded burn times of 100 – 330 s, which can cause flight times of 200 – 600 s, excluding outliers; and the NFCPSA reported flight times of 120 – 300 s.) It is also possible that the sky lanterns were not released precisely when they were neutrally buoyant in the NFCPSA experiments.

Figure 7 shows the duration of the flights for each of the sky lantern types. Generally, the total flight times were greater than the flame-out times, which gives some confidence that in ideal operating conditions (still air, properly protected fuel cells, lit according to the manufacturers' instructions), the likelihood of open flame contacting flammable substances or materials on the ground are minimal.

However, some tests produced outliers, for instance, the sky lanterns with slow or delayed ignition due to the uneven burning of the fuel patch, or the rupture in one of the Type E envelopes. In one experiment, the sky lantern ascended with a nominal profile, but 105 s into the experiment, the crown of the sky lantern caught fire, which

burned a hole approximately the diameter of the bottom opening through the top, which suddenly released the stored hot air, and the sky lantern would have crashed to the ground – while the fuel cell was still lit. Therefore, there will always exist a non-zero probability that a burning fuel patch from a sky lantern could come into contact with combustibles. Again, it is noted that the *in situ* results from the NFCPSA may lead to more accurate performance and duration measurements. Many factors of the common operating conditions, such as lateral wind speed, may affect the height and duration of the flight, and may lead to an open flame coming into contact with trees, grass, or other combustible material.

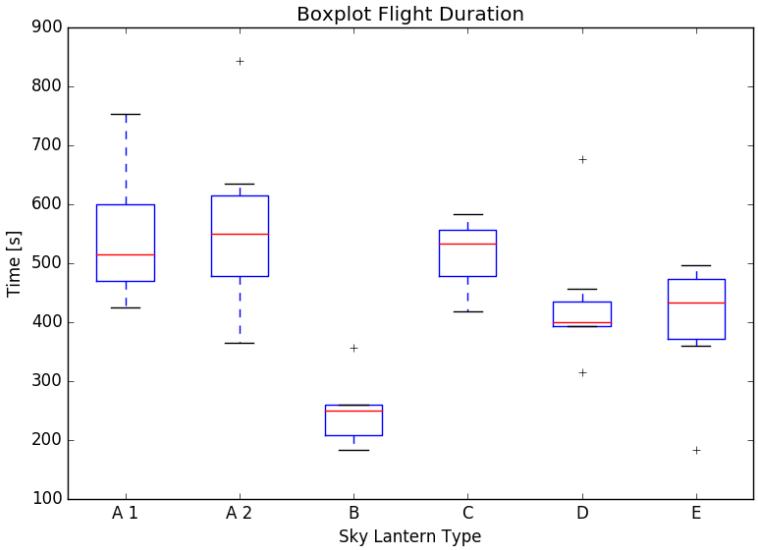

Figure 7. Boxplot of sky lantern type and calculated flight duration

VIII. Conclusion

Using buoyancy and ideal gas formulas from lighter-than-air balloon literature, and standard equations of motion, a mathematical model describing the sky lantern flight profile was created. By combining the quantitative measured data with the mathematical model, the vertical flight profile of five types of sky lanterns was calculated. It was concluded that the flight profile of the sky lantern could enter the range of low-flying aircraft or unmanned aerial vehicles. Apart from one case in which the impregnated rice paper envelope combusted, the flight durations for the five types of sky lanterns were all sufficient to prevent open flame fuel patch contact with the ground.

During this research, it was found that there was a large variability of mass and manufacturing quality between the different sky lantern types. Both the burner and the envelope mass were not uniform and, as a result, similar type sky lanterns had between 5 and 10% total mass difference. The effect of the mass variation on performance was noticeable, particularly between the similarly shaped sky lanterns. The shape of the sky lantern also influenced the maximum recorded height calculated by the model, although assumptions were made in the model that neglected the influence of shape on the aerodynamics. As such, the range in performance is widespread, and the altitude performance was not validated experimentally with *in-situ* testing. These factors should be considered when using the current model and its results.

More research is required characterize the assumptions better made in this paper (such as a constant drag coefficient, or the simplifying assumptions in the mathematical model) and include external properties (temperature, density) with envelope thermodynamics, to increase model fidelity. In the future, a full-scale verification and validation of the sky lantern model performance is planned to improve model quality.

Acknowledgments

The authors would like to thank the Delft Aerospace Structures and Materials Laboratory (DASML) staff for their support in developing and executing the sky lantern static tests.

References

[1] Federal Aviation Administration, "Title 14 Code of Federal Regulations (14 CF) Part 31 Airworthiness Standards: Manned Free Balloons", 1964.
[2] Federal Aviation Administration, "The Code of Federal Regulations (CFR) Part 101 Subpart D", 1964
[3] Voedsel en Waren Autoriteit, ”Verkenning van de veiligheid van wensballonnen”, ZW 09231d, 2009.
[4] Kreider, J. F., “Mathematical Modeling of High Altitude Balloon Performance,” AIAA Paper 75-1385, 1975.
[5] Stefan, K. "Performance Theory for Hot Air Balloons", Journal of Aircraft, Vol. 16, No. 8 (1979), pp. 539-542.
[6] Morris, A. L., "Scientific Ballooning Handbook," National Center for Atmospheric Research, Boulder, CO, NCAR-TN/IA-99, May 1975.
[7] Tuhin Das, T., Mukherjee, R., Cameron J., “Optimal Trajectory Planning for Hot Air Balloons in Linear Wind Fields”, Journal of Guidance, Control, and Dynamics, Vol. 26, No. 3 (2003), pp. 416-424.
[8] Ellenrieder, T. “The Modelling and Validation of the Vertical Dynamics of a Hot Air Balloon”, Journal of Aerospace Engineering 1999, 213 (G1), 57–62.